

Minoru Kubota

Quantized vortex state in hcp solid ^4He

July 24, 2018

Keywords solid He · vortex state · vortex fluid state · supersolid state

Abstract The quantized vortex state appearing in the recently discovered new states in hcp ^4He since their discovery^{1,2} is discussed. Special attention is given to evidence for the vortex state as the vortex fluid (VF) state^{3,4,5,6} and its transition into the supersolid (SS) state^{7,8,9}. Its features are described. The historical explanations^{10,11,12,13,14} for the SS state in quantum solids such as solid ^4He were based on the idea of Bose Einstein Condensation (BEC) of the imperfections such as vacancies, interstitials and other possible excitations in the quantum solids which are expected because of the large zero-point motions. The SS state was proposed as a new state of matter in which real space ordering of the lattice structure of the solid coexists with the momentum space ordering of superfluidity. A new type of superconductors, since the discovery of the cuprate high T_c superconductors, HTSCs¹⁵, has been shown to share a feature with the vortex state, involving the VF and vortex solid states. The high T_c s of these materials are being discussed in connection to the large fluctuations associated with some other phase transitions like the antiferromagnetic transition in addition to that of the low dimensionality. The supersolidity in the hcp solid ^4He , in contrast to the new superconductors which have multiple degrees of freedom of the Cooper pairs with spin as well as angular momentum freedom, has a unique feature of possessing possibly only the momentum fluctuations and vortex ring excitations associated with the possible low dimensional fluctuations of the subsystem(s). The high onset temperature of the VF state can be understood by considering thermally excited low D quantized vortices and it may be necessary to seek low dimensional sub-systems in hcp He which are hosts for vortices.

PACS numbers: 67.80.bd 67.25.dk 67.25.dt 67.85.De

Institute for solid State Physics, the University of Tokyo,
Kashiwanoha 5-1-5, Kashiwa, 277-8581, Japan
Tel.: -81-4-7136-3355
Fax: -81-4-7136-3355
E-mail: kubota@issp.u-tokyo.ac.jp

1 Introduction

Quantized vortices are the essence of superfluidity¹⁶ and superconductivity (superfluidity of electrons). They originate in the coherence of the wave function describing the system over macroscopic length scales much larger than the vortex core sizes. In the "classical" superfluids, the macroscopic coherence has been provided by the Bose-Einstein Condensation (BEC) of the constituent Bose particles¹⁷, and that of Cooper pairs¹⁸, in the case of Fermion systems. The superfluid-normal fluid transition has been discussed since the classical discussion by Feynmann¹⁹ as a phase transition by the destruction of the macroscopic coherence by excitations of quantum vortex loops, and it is discussed much more concretely by a simpler vortex rings model by Williams²⁰. More recently, since the discovery of the cuprate high T_c superconductors, HTSCs¹⁵, people realized that we do have the quantized vortex state, which is characterized by the complex $T - H$ phase diagram of the new superconductors, namely, a VF state and different types of vortex solid states have been realized. All the "new type of superconductors" possess a common feature, namely the unique vortex state²¹. It is also true for the newly found FeAs based superconductors²². Early discussions for the vortex state in the cuprates argued for the importance of the 2D character of the CuO_2 plane Cooper pairs for the cuprate HTSCs²³. This kind of appearance of the vortex state in the new superconductors, the strongly correlated electron systems, is often discussed nowadays in connection to the 2D pancake-type vortices²⁴, but is never discussed for any mass superfluidity nor for the physics of solid He with a single exception²⁵, though solid He is actually a candidate for being one of the most strongly correlated systems.

Ideal 2D superfluidity and the physics of 2D vortices had been discussed for the superfluidity of the 2D ^4He films by Berezinskii²⁶, Kosterlitz and Thouless²⁷ and lead to the idea of topological BKT phase transition, where real BEC is absent, but 2D quantized vortices and local condensate were implicitly supposed. Its unique features, the 2D density linear transition temperature T_{KT} and the universal jump²⁸ in the superfluid density are clearly experimentally confirmed^{29,30}. A detailed discussion of the dynamics of the KT systems was given by Ambegaokar, Halperin, Nelson, and Siggia³¹. KT superfluidity of the CuO_2 plane electron Cooper pairs and Josephson coupling between the layers are the essence of the HTSC vortex physics. A unique vortex state, first discussed for the cuprate HTSCs supposes thermal excitations²³ of low dimensional quantized vortices, which have low enough energy and high entropy in high fields.

Readers are recommended to refer to a longer paper by the present author on the vortex physics in hcp ^4He (I), which includes a discussion on the essence of superfluidity and the vortex physics in 3D He film systems, where detection of 3D vortex lines penetration by torsional oscillator (TO) technique is also described³².

2 "Possible supersolidity" and Quantized vortex physics in hcp ^4He

The discussion of possible superfluidity in the quantum solid, the SS state, had historically assumed a non-negligible amount of vacancies, interstitials, and other possible excitations in the quantum solid^{11,12,13}, because of the zero point motions in such systems and the possible Bose Einstein condensation BEC of these quasi

particles or excitations. It was believed to certainly occur at some sufficiently low temperature. In 1970 no other possible mechanism for superfluidity in the solid was known. The BKT mechanism^{27,28,29,31} for a 2D system was first introduced in 1972 and the lack of knowledge of other mechanisms like those possible in 1D systems lead to this situation. It was later when a 1D dislocation network was considered as a candidate explanation for a possible SS state^{33,34}.

New development started when Kim and Chan reported their new experimental results using torsional oscillator TO technique,^{1,2} which raised the question whether or not they finally found the long sought, non-classical rotational inertia, *NCRI*¹³ of the SS state. There have been frequent international workshops since 2006 when other groups started confirming results, yet the system remains still mysterious even after so many years of work by an increasing number of groups. By now several reviews^{35,36,37,38} have appeared since the restart by Kim and Chan^{1,2}. The main problem is that nobody knows what a SS state should look like. There are plenty of interesting aspects of the solid as well in the quantum solid He. First of all, Day and Beamish³⁹ reported an increase of the shear modulus towards lower temperatures near 200 mK, almost the same temperature range as TO anomalies had been reported. Substantial change of the properties by a minute amount of ³He is also reported since the beginning¹. A more detailed discussion of these peculiar behaviors is left for later in the discussion chapter. In the present chapter discussion is concentrated on the problem of whether quantized vortices are present in the system or not and if there is enough evidence supporting supersolidity and related phenomena in solid He.

Our discussion started with solid He, but now we limit ourselves to the hcp phase of the solid ⁴He, because of the following development: The shear modulus increases below around 200 mK for hcp ⁴He³⁹. A similar change was also found⁴⁰ in hcp ³He, but the TO response was found only in hcp ⁴He.

2.1 Quantum Vortex State in hcp ⁴He

Although enough details of the microscopic mechanism responsible for what is occurring in hcp ⁴He are still not available to explain all the all the experimental observations, the existence of quantized circulations or quantized vortices can be shown by experimental evidence and it should be regarded as fundamental to determine the direction of the research activities. In this chapter experimental discoveries are discussed which are supporting quantized vortices in the VF state in hcp solid ⁴He, a unique state among all the known superfluids. It is, however, quite common to discuss the VF state^{3,4} in the so called "new type of superconductors"^{41,42}, though there have not been many microscopic arguments from the standpoint of quantized vortices in the new type of superconductors. Anderson²⁵ has recently proposed an explanation which may cover a large portion of various experimental observations starting from the VF state picture.

The next subsection of this chapter starts with experimental discoveries of the peculiar TO drive velocity V_{ac} dependence observed in hcp solid ⁴He (Fig. 1), which turned out to indicate the unusual behavior of the VF state and that of onset of the VF state. Subsection 2.3 deals with vortex dynamics in the VF state, utilizing the standard theoretical method of handling the tangled vortices in superfluid turbulence⁶. In chapter 3 the recent discovery of the transition from the VF state

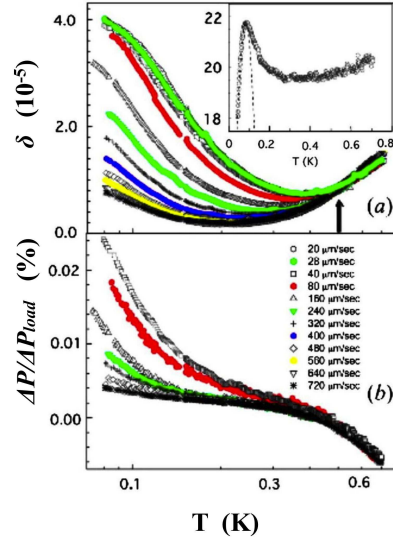


Fig. 1 T dependence of reduced energy dissipation δ (a) and $\Delta p/\Delta p_{load}$ (b) at various edge velocities V_{ac} in $\mu\text{m/s}$ for a 32 bar sample⁵. The values of δ are presented without any artificial shift of data, which has often been needed in other papers. Careful treatment of the cryostat is essential. Some data are omitted for clarity [all of the data on V_{ac} dependence are plotted in Fig.2 of Penzev *et al.*⁵(a) and (b)]. An arrow in (a) indicates T_o , across which V_{ac} dependence changes. The inset in (a) indicates a typical dissipation peak with higher T_p . The low T part of the peak was fitted with a Gaussian function. The zero of $\Delta p/\Delta p_{load}$ in (b) is taken where V_{ac} dependence disappears near T_o .

into the real SS state^{7,8,9} is reported and its properties are discussed in terms of the SS density ρ_{ss} and the critical velocity V_c .

2.2 Discovery of the onset temperature T_o of the Vortex Fluid(VF) State in hcp ^4He and its unique properties

Actually the vortex phase diagram of hcp ^4He was first experimentally proposed by reporting a definite onset temperature by Penzev *et al.*⁵, after Anderson's suggestion^{3,4} and by describing unique features of the VF state, which appeared to be characterized by thermally excited vortex fluctuations⁶. These thermally excited fluctuations cause the unique drive amplitude dependence of the TO response⁵. Fig 1 shows a detailed study of hcp ^4He at T above the dissipation peak at T_p . The V_{ac} at the outer edge of the cylindrical sample influences both Period P shift $\Delta P/P_{load}$ and energy dissipation in the sample δ quite a lot, but only below an "onset temperature" T_o . As noted before, although this strong V_{ac} dependence was reported even in the original work by Kim and Chan¹ nobody discussed quantitatively its dependence, but refer to it as a sort of "critical velocity" phenomenon. This speed, on the order of $10\mu\text{m/s}$, needs to be discussed as a characteristic speed⁵ to describe system size fluctuations instead of a "critical velocity" in the later section on vortex dynamics in the VF state. The VF state may not have a

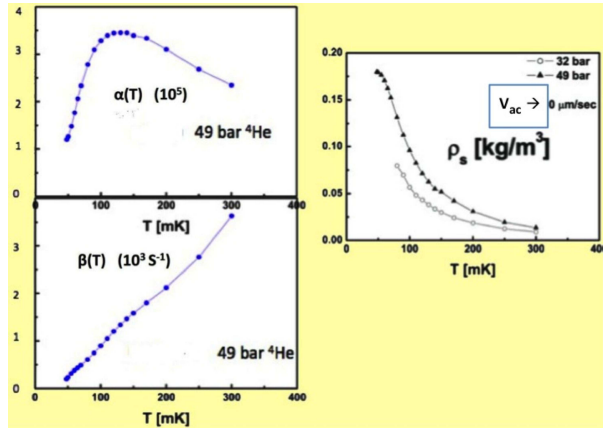


Fig. 2 Parameters $\alpha(T)$, $\beta(T)$, and $\rho_s(T) = NLR(S(V_{ac} \rightarrow 0))$ obtained from the data of Fig. 1 of Nemirovskii *et al.*⁶ with the use of analysis described in text. $\beta(T)$ goes to zero, in other words, it means the relaxation time goes to infinity at extrapolated $T \approx 30$ mK. This may imply the possible disappearance of the thermal excitations and of the VF state.

critical velocity. In the "onset" paper⁵ the authors discussed T_o as the onset temperature of the VF state, below which quantized vortices are thermally excited and that $NLR(S)$ exhibits a unique temperature dependence, which is different from any of the order parameters below a phase transition. Furthermore, they observed rather clear $\log(V_{ac})$ linear behavior^{43,5} (see also Fig 8) over a decade of V_{ac} for the entire T range well above the dissipation peak at T_p . This dependence is argued to be responsible either for appearance of the quantized vortex lines penetrating the sample, or polarizing the vortex rings in the VF state, in both cases, thereby reducing the disorder of the thermally excited VF state. This observation is unique compared with all other TO or other oscillator experimental results for known superfluid transitions, KT transition of 2D films^{29,30}, bulk He liquids in Vycor⁴⁴, and also in the artificial 3D superfluid made of ⁴He monolayer superfluid films^{45,46,32}, where energy dissipation ΔQ^{-1} is larger when the oscillation amplitude is driven larger. Their intuitive discussion is also proven in terms of vortex dynamics in the randomly fluctuating vortex tangle⁶. The transition into the SS state^{7,8} will be discussed, which is characterized by a unique order parameter and the critical velocity in the next chapter 3.

2.3 Vortex dynamics in the VF state and possible disappearance of the thermal excitations

The VF state has been discussed with regard to the H-T phase diagram of the new type of superconductors since discovery of the cuprate HTSCs, yet, there has not been a quantitative discussion from the quantized vortex dynamics viewpoint. There are, however, arguments developed for the vortex dynamics in the superfluid turbulence, which often deals with physics at $T=0K$, where no thermal excitations exist. The superfluid turbulence state is excited by various methods, but it is excited by some external flow velocity exceeding a characteristic critical velocity.

The VF state, on the other hand, is excited by thermal energy and it is considered that the thermal energy can exceed the critical velocity of the turbulent state for the vortex tangle in the VF state. As has been seen in the previous section, a peculiar feature of the VF state of hcp He is that some fluctuations can be reduced by the TO drive excitations⁵, namely larger drive velocity reduces the fluctuating signal more than smaller drive excitations, as can be seen in Fig 1 and Fig 4, for example. This is actively studied and there are references for it. Nemirovskii *et al.*^{8,6}, consider quantized vortex element dynamics for the experimental data analysis of the TO responses of the VF state in hcp ⁴He, using a phenomenological relaxation model;

Angular momentum of the superfluid fraction appears only due to the presence of either aligned vortices (vortex array) or the polarized vortex tangle having nonzero total average polarization $P = L \langle s'(\xi) \rangle$ along the applied angular velocity Ω (axis z, the magnitude of $\Omega = V_{ac}/R$, where R is radius of the sample). Here L is the vortex line density (total length per unit volume), $s(\xi)$ is the vector line position as a function of label variable ξ and $s'(\xi)$ is the tangent vector. In the steady-state case there is a strictly fixed relation between the total polarization $L \langle s'(\xi) \rangle$ and applied angular velocity Ω ,

$$\Omega = \kappa P/2 = \kappa L \langle s'(\xi) \rangle / 2. \quad (2.1)$$

They^{8,6} pointed out that there are two possible mechanisms for relaxation-like polarization of the VF. The first is alignment of elements of the vortex lines due to interaction with the normal component (see Tsubota *et al.*(2004)⁴⁷ for detailed explanation). This interaction (mutual friction) is proportional to the local normal velocity, which in turn is proportional to the rim velocity V_{ac} . Thus it is natural to suppose that polarization P of the vortex tangle due to alignment of filaments along $\Omega(t)$ occurs with typical inverse time $\tau^{-1}(V_{ac})$ which is proportional to the rim velocity V_{ac} . Let us illustrate according to Nemirovskii *et al.*, with consideration of Tsubota *et al.*(2004)⁴⁷. In the presence of mutual friction there is a torque acting on the line and the angle ϕ between axis z and the line element changes according to the equation $d\phi/dt = \alpha(V_{ac}/R) \sin\phi$ (α is the friction coefficient, dependent, in general, on T and pressure p). Except for a short transient, the solution to this equation can be described as a pure exponential $\sim \exp(-t/\tau_1(V_{ac}))$, with the velocity dependent inverse time $\tau_1^{-1}(V_{ac}) \sim \alpha(V_{ac})/R$. Thus, it is concluded that during time-varying rotation or torsional oscillation vortex filaments tend to align along the angular velocity direction. However, there can be not enough pre-existing vortex lines in the tangle to involve all the superfluid part into the rotation to satisfy the relation (2.1), or on the contrary the initial vortex tangle can be excessively dense.

In such a case deficit (extra) vortices should penetrate into (leave from) the bulk of the sample. This penetration occurs in a diffusion-like manner⁴⁸ and leads to the relaxation-like saturation of the vortex line density $L(t)$ Nemirovskii *et al.*^{8,6} assume that this saturation occurs in an exponential manner with some characteristic inverse time $\tau_2^{-1} = \beta$. Due to linearity of the diffusion process it is supposed that the coefficient β is velocity independent, but can be a function of T and P . Combining these two mechanisms it is assumed that the total polarization of the VF occurs in a relaxation-like manner with a pure exponential function $\phi(t'/\tau) \sim$

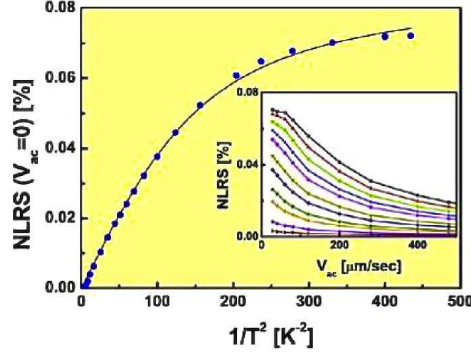


Fig. 3 $NLRs_0(T)=\Delta P/\Delta P_{load}$ at $V_{ac}\rightarrow 0$, (It may be called ρ_s of the VF state to distinguish it from the supersolid density ρ_{ss}) is displayed⁷ as a function of $x = 1/T^2$. The solid line through data points is the Langevin function $f(x) = a[\coth(bx) - 1/(bx)]$ with $a = 0.0878 \pm 0.0011$, and $b = 0.0148 \pm 0.0004$. The inset shows the V_{ac} dependence of the data at ten temperatures below 300 mK, for clarity on linear scales. It can be safely extrapolated to $V_{ac}\rightarrow 0$. See for details Fig.2 of Penzev *et al.*⁵.

$\exp(t'/\tau)$. The inverse time τ^{-1} of relaxation is just the sum of $\tau_1^{-1}(V_{ac})$ and τ_2^{-1} :

$$\tau^{-1} = \alpha(T)V_{ac}/R + \beta(T). \quad (2.2)$$

The parameters α , β , and $\rho_s(T) \equiv NLRs_0(T) = \Delta P/\Delta P_{load}$ at $V_{ac}\rightarrow 0$, obtained using experimental data analysis for a 49 bar hcp ^4He sample, are given in Fig. 2. The ΔQ^{-1} and $NLRs$ at different T could be well reconstructed from these parameters and plotted in Fig. 3 of Nemirovskii *et al.*⁶. $\rho_s(T)$ can be regarded as the VF state SS density and it will be contrasted with the real SS density $\rho_{ss}(T)$ which will be discussed in chapter 3.

Now let us consider what all these results of the measurements as well as the data analysis mean. An interesting observation of Fig. 2 α and especially β is that they are approaching zero when T approaches about 30 mK while ρ_s is gradually increasing towards lower temperatures. That means the relaxation time τ is becoming infinite and vortices are becoming difficult to move, while ρ_s is high. This situation reminds us of the dissipation peak appearing near the KT transition³¹, where it is interpreted that the thermally excited 2D vortices loose number density rapidly and the dissipation peak is localized near the transition at T_{KT} , while the superfluid density remain towards $T=0$. The VF state may have lost the thermal activation below $T \sim 30$ mK.

Another interesting observation for the VF state of hcp ^4He is expressed in Fig. 3. The $\log V_{ac}$ linear behavior at larger V_{ac} values than about $40 \mu\text{m/s}$ linear velocity has been already discussed, and now let us look at the situation when V_{ac} approaches zero. The line through the data points in Fig. 3 is the Langevin function with $x = 1/T^2$, $f(x) = a[\coth(bx) - 1/(bx)]$ with $a = 0.0878 \pm 0.0011$, and $b = 0.0148 \pm 0.0004$. Various other possible fits were tried, but they failed, for example, with $x = 1/T$. The origin of this interesting temperature dependence is not yet known. Actually this $1/T^2$ dependence appears repeatedly in the following analysis as well. The Langevin function with $x = 1/T$ is followed by the generalized

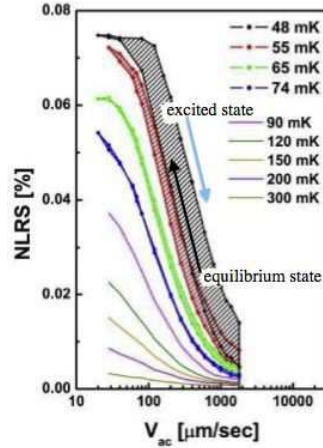


Fig. 4 The $\log(V_{ac})$ dependence of $NLRS = \Delta P / \Delta P_{load}$ of our solid ^4He sample at 49 bar at constant temperatures as given in the figure. Measurements were performed at each T starting at the largest drive which corresponds to $1,800 \mu\text{m/s}$ and then to lower drive velocity, stepwise. After reaching the minimum drive velocity measurement at $\sim 27 \mu\text{m/s}$ and after observing equilibrium, then upwards at each T for the remaining measurements. Appearance of the hysteretic behavior is found starting at 74 mK and lower temperatures. Limited data are shown for clarity.

susceptibility of an ensemble of classical dipoles with fixed number. It is not clear if the good fit is just accidental or not.

If one were to consider the 3D counterpart^{3,4} of BKT theory^{26,27}, one would need to consider the behavior of the ensemble of vortex rings, which are thermally excited in local domains, and a transition into the SS state would occur because of the coherence length growth towards zero temperature of the low dimensional subsystems, just as in the 3D superfluid made of He films^{45,46}.

3 Discovery of the transition into the SS state from the VF state in hcp ^4He : Hysteresis found below a fixed temperature, T_c

When Anderson proposed the vortex fluid state to explain the reported experimental observation until that time, he pointed out that the real SS state transition should be located at much lower temperature^{3,4}.

The occurrence of the unique hysteresis in the TO experiments with solid ^4He samples when the excitation velocity V_{ac} was changed at low temperature had been reported first by Kojima's group,⁴⁹ and then by Chan's group,⁵⁰ and then by Reppy's group.⁵¹ They could not determine that the hysteresis is connected with a definite transition at a fixed temperature. Shimizu *et al.*,⁷ found for the first time that the hysteresis occurs below a characteristic temperature T_c in solid He. They^{8,7,9} propose from their detailed study of the hysteretic behavior that the hysteretic component of the $NLRS$, $NLRS_{hys}$ is actually additive to the $NLRS$ quantity of the VF state. $NLRS$ is found to continue to grow towards lower temperatures from the onset temperature T_o as shown in Fig. 1. It has a unique, continuous temperature dependence towards $T = 0$ K as depicted in Fig. 3. The additive behavior

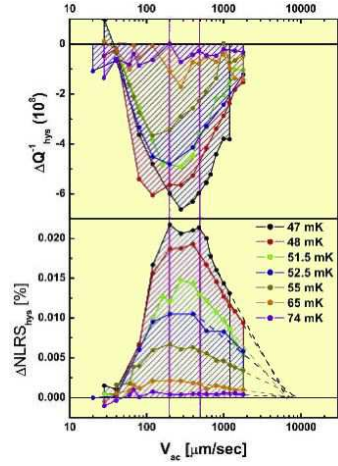


Fig. 5 The hysteretic components of the TO responses, ΔQ_{hys}^{-1} as well as $\Delta NLRShys = NCRIF$ are plotted against $\log V_{ac}$. The hysteretic behavior starts at $V_{ac} \sim 40 \mu\text{m/s}$ at all temperatures below ~ 75 mK. Both $\Delta NLRShys$ and ΔQ^{-1} reach some extreme values for the range $V_{ac} = 200 - 500 \mu\text{m/s}$. Then the absolute size of both quantities starts to decrease. Nearly $\log V_{ac}$ linear decreases were observed, especially for $\Delta NLRShys$. From this straight extension of the $\log V_{ac}$ linear dependence, a critical velocity, ~ 1 cm/s, to suppress the $NCRIF = \rho_{ss}$ to zero, was obtained, which compares well within an order of magnitude with $V_c = h/(m_4 \xi_0 \pi) = 6 - 12$ cm/s, for $\xi_0 = 25 - 50$ nm; see text.

of the hysteretic component can be also seen in Fig. 4. . The expected SS state should be characterized by a definite order parameter, supersolid density ρ_{ss} , in addition to a critical velocity v_c to destroy this state. These points are discussed in much more detail in the following section.

3.1 Hysteretic component of the TO responses and possible SS density

As pointed out above, the hysteretic components of the TO response are found to be additive to the response of the VF state. See Fig. ?? Shimizu *et al.*,⁷ as well as Kubota *et al.*,^{8,9} tried to analyze the hysteretic components separately from those for the VF state. Fig. 5 shows the dissipation change ΔQ_{hys}^{-1} (upper column) and the $\Delta NLRShys$ change across the hysteresis vs $\log V_{ac}$ (lower column). The lower branch of the $NLRShys$ is named as the "equilibrium" state and the upper branch as the "excited" state branch. Fig. 5 shows the difference between the "excited" state and "equilibrium" state. The actual experimental method is described in detail in Kubota *et al.*,⁹. Measurements are performed at a fixed temperature and after equilibrium is established first at high V_{ac} of the TO and then going to lower excitations, step wise after reaching "equilibrium" or steady state at each step, to the lowest AC velocity on the order of 8 to $30 \mu\text{m/s}$. Then V_{ac} is increased, also stepwise, up to the maximum speed $1,800 \mu\text{m/s}$.

What is observed in Fig. 5 is a characteristic V_{ac} value of about $40 \mu\text{m/s}$, above which hysteretic components develop. $NLRShys$ reaches a maximum value at 200

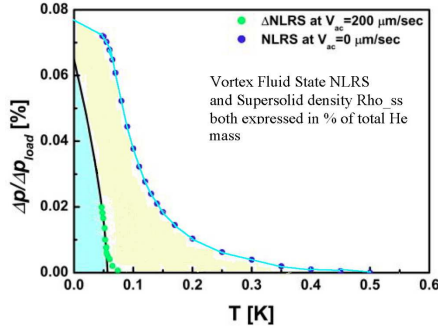


Fig. 6 $NLRS = \Delta P / \Delta P_{load}$ of the vortex fluid (VF) state expressed in % of He mass^{7,8,9} and the hysteretic component of $NLRS$, $\Delta NLRS_{hys}$, which is assumed to be the SS density ρ_{ss} , as a function of T (for details⁹). At the high temperature end, $NLRS$ behaves as $1/T^2$, whereas ρ_{ss} starts below T_c and increases towards $T=0$. The latter behaves as an order parameter unlike the $NLRS$. The behavior of the $NLRS$ in the VF looks 'paramagnetic', with a Langevin function modified with $x = 1/T^2$. Langevin function behavior is expected for the susceptibility of an ensemble of classical dipoles, usually with $x = 1/T$. Arranged from Fig.2 of Kubota *et al.*⁸.

$\mu\text{m/s}$ and then stays almost constant until about $500\mu\text{m/s}$ and then it decreases almost linearly in the semi log plot as in Fig. 5. With linear extrapolation in the semi log plot of the figure, it is observed that the $NLRS_{hys}$ component disappears at V_{ac} about $10,000\mu\text{m/s}$ or 1 cm/s . A critical velocity V_c may have been found to destroy the $NLRS_{hys}$ component. While $NLRS$ increases when it is converted to the excited state, ΔQ_{hys}^{-1} shows negative changes. This negative change indicates dissipation in the "excited" state is less than in the "equilibrium" state and implies that vortices are expelled from the sample. Shimizu *et al.*⁷, as well as Kubota *et al.*^{8,9}, plotted the maximum of this $NLRS_{hys}$ (at $V_{ac}=200\mu\text{m/s}$) as a function of temperature together with the $NLRS$ extrapolated to $V_{ac} = 0$ in Fig. 6. While $NLRS$ of the VF state gradually appears as $1/T^2$ below $T_o \sim 500\text{ mK}$, the hysteretic component $NLRS_{hys}$ (at $V_{ac}=200\mu\text{m/s}$) starts to appear much more sharply below the temperature $T_c = 75\text{ mK}$ and then changes slope around 60 mK .

Furthermore, they^{7,9} checked this $NLRS_{hys}$ (at $V_{ac}=200\mu\text{m/s}$) in various ways and found an interesting feature that they could fit as $(1-T/T_c)^\gamma$ with $\gamma=2/3$ by choosing $T_c=56.7\text{ mK}$. This is the critical behavior expected for a 3D superfluid transition described with 3D XY model. Using the Josephson's length relation^{52,53,54} $\xi = \kappa k_B T_c / \rho_s$, one can evaluate the coherence length for the SS state as plotted in Fig. 7, for the hcp He 49 bar sample as a function of reduced temperature, $1 - T/T_c$ with $T_c=56.7\text{ mK}$. The inset of the figure compares the Josephson's coherence length ξ for the VF state $NLRS$ and for the SS state $NLRS_{hys}$ (at $V_{ac}=200\mu\text{m/s}$). It is seen that the coherence length evaluated in the same manner differs for the VF state and for the SS state. The former is shorter for the same temperature. This may give some clue for the relation between the VF and the SS states, namely the SS state develops a macroscopic scale coherence, while the length of the VF state coherence is limited. From all of these trials, it is proposed that $NLRS_{hys}$ (at $V_{ac}=200\mu\text{m/s}$) is actually the real SS density ρ_{ss} . This proposal will be considered later once again in connection with vortex lines penetration phenomena under DC rotation. In connection to the above question of the relation

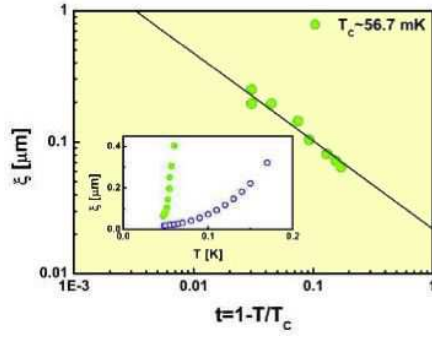


Fig. 7 Critical behavior of ξ obtained from the data in Fig. 4. $T_c = 56.7$ mK was chosen, supposing $\rho_{SS} = (1-T/T_c)^\gamma = t^\gamma$ with $\gamma=2/3$. $\xi_0 \sim 25 - 50$ nm was obtained by simple extrapolations, horizontal and straight extension to $t=1$ or $T=0$ K. Inset shows ξ for the SS, ξ_{SS} , as well as for the VF state, ξ_{VF} (open circles), with linear scales. $\xi_{SS} > \xi_{VF}$ at all T where they coexist.

between the VF state and the SS states and the transition between them, the details of the VF state *NLRS* behavior as a function of V_{ac} will be checked once again in the next section.

3.2 Further detailed study of the $\log V_{ac}$ linear dependence study of the VF state *NLRS* and transition into the SS state

Having seen that the hysteretic behavior starts at a finite temperature and the excited state shows a higher value of the *NLRS* than the equilibrium state, which seems to be a continuation of the VF state from higher temperatures to lower temperatures, it is questioned if the VF state itself may undergo some change at T_c . Kubota *et al.*⁹ studied in detail the V_{ac} dependence of the *NLRS* in the "equilibrium" state. Fig. 8 shows a $\log V_{ac}$ linear relation over a decade of V_{ac} value for each of given T . It then changes slope and again follows a $\log V_{ac}$ linear relation for each temperature studied between 50 mK and 300 mK. The slope of the $\log V_{ac}$ linear relation for each temperature was plotted versus a variety of temperature functions and an interesting relation was found for the slope as well as the turning point for *NLRS* as seen in the plot in Fig. 9. It was found that the initial slope varies linearly with $1/T^2$ dependence and then it makes a jump and continues to follow another linear relation, whereas the $NLRS_{turning}$ point value is also found to follow a linear relation over some $1/T^2$ range and then jumps to another linear relation. The jump is happening at $1/T^2 = 0.00025 \pm 0.0004 K^2$, or $T = 59 - 69$ mK, which coincides with the T_c within the error.

Actually the $\log V_{ac}$ linear dependence may be expected, as originally pointed out by Anderson³, if a tangled quantized vortex state is to be polarized by the excitation or to form linear vortex lines so this result may be related to the polarizability change in the VF state at T_c in addition to the hysteretic component appearance discussed in section 3.1. There remains a question as to the origin of the peculiar $1/T^2$ dependence. Anderson⁵⁵ pointed out that it may be related to a quantum phase transition, but it needs further study.

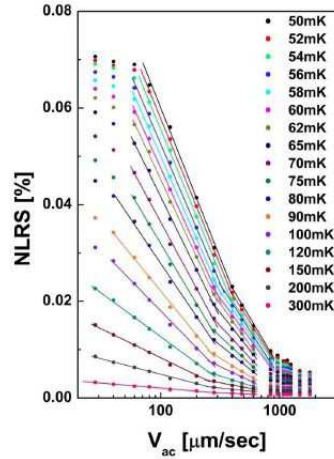


Fig. 8 Detailed data of $NLRs$ of hcp ^4He 49 bar sample, as a function of $\log V_{ac}$,^{7,9}. It is observed that the $\log V_{ac}$ linear relation is followed over some range of V_{ac} , starting at a certain V_{ac} value. Then some other $\log V_{ac}$ linear like dependence appears at a higher V_{ac} range for each of data at a T . Expanded details are discussed by Kubota *et al.*⁹, in its Fig.4.and 5. The $\log V_{ac}$ linear relation was discussed for solid ^4He first by Anderson^{3,4} as evidence of quantized vortex lines involvement in the physics of solid ^4He , and then was experimentally demonstrated by Penzev *et al.*⁵ for polarizing a tangled state of the VF state.

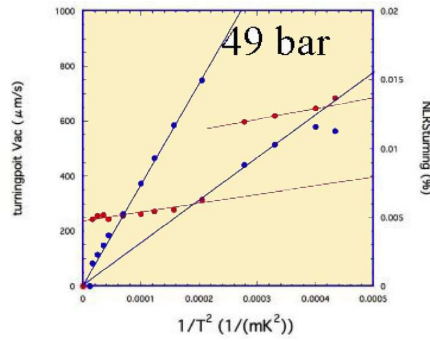


Fig. 9 The turning point values of $NLRs$ as well as those of the velocity V_{ac} are plotted vs $1/T^2$. The turning point seems to show considerable regularity. A transition was found at $1/T^2 = 0.00025 \pm 0.00004 \text{ K}^2$, or $T = 59\text{--}69 \text{ mK}$, which coincides with other T_c determinations.

4 Experimental evidence for the quantized vortex lines penetration into the SS state under DC rotation

Straight quantized vortex lines are introduced into a macroscopic coherent state of a superfluid in a cylindrical vessel under DC rotation above a certain angular velocity Ω_{c1} ⁵⁶, and at large enough $\Omega \gg \Omega_{c1}$, the number of vortices would be changing in proportion to the angular velocity Ω , $n_v \propto \Omega$ until it comes close to Ω_{c2} , which is usually far beyond experimentally achievable speed of rotation in the roughly centimeter sized vessels used for the bulk ^4He . One needs a much

larger size for the vortex core than $10 \mu\text{m}$ to reach the condition beyond Ω_{c2} ⁵⁷. The state beyond Ω_{c2} means that vortex cores overlap each other and destroy the superfluidity of the dimensionality defined for the vortex core. It may not necessarily destroy all the coherence of the system, but that of the dimension to which the vortex core is connected. In the present discussion of rotation in a 3D system, DC rotation beyond $\Omega_{c2}(3)$ would destroy the 3D superfluid state. This consideration becomes important when various dimensional subsystems are involved in a single superfluid system. For example, the 2D vortex core diameter is found to be 2.5 nm for the monolayer film superfluid⁵⁸ and there is an independent 3D vortex core size which is found to be determined by the controlled pore size of the porous glass substrates⁵⁴. It had been proposed to detect vortex lines through the SS state of solid ^4He by TO technique, observing the fact that solid ^4He also shows evidence of thermal excitations, namely the dissipation peak, presumably vortex rings excitations⁵⁹.

An experimental tool to realize vortex lines penetration is rotation of the vessel. The ISSP high speed rotation cryostat (ISSP-HSRC), with which vortex penetration as well as rejection phenomena are being studied in the SS state of hcp ^4He , is described in Yagi *et al.*⁶⁰. It also reviews how vortex lines in different superfluids have been observed and discusses features of the ISSP-HSRC in detail.

Since the first report by Kim and Chan, one of the most specific features of the solid He TO responses is the sensitivity to minute AC speed, V_{ac} on the order of $10 \mu\text{m/s}^{1,2}$. It is the linear edge speed which seems to be important and not amplitude or acceleration according to Aoki, Graves, and Kojima⁴⁹. The sensitivity to the linear velocity of the TO responses is also reproduced in our measurements (Fig. 1, Fig. 4, and so on). Based on these observations it is essential to minimize the variations in the rotational speed, in addition to the direct vibrations of the TO itself, for the successful TO study of solid ^4He . This is easily seen by taking a 10 mm inner diameter torsion bob in which sample He is contained and DC rotational speed of 1 radian/sec with 10^{-3} stability. This situation alone would already cause variations on the order of $6.3 \mu\text{m/s}$ linear velocity in addition to the usual V_{ac} . This size of AC velocity change would already cause significant modification of the TO responses. One needs to be concerned about actual stability of the rotational speed apart from the average drive velocity accuracy. If the sample diameter were larger then the linear velocity effect would be further enlarged and would easily cause misleading TO results under DC rotation. There is some idea of the constancy of ISSP rotating cryostats DC angular speed since they have been performing both dilution refrigerator temperature TO experiments on solid He and nuclear demagnetization T range experiments on superfluid ^3He ^{61,62}. They record heat leak under DC rotation on the order of 10 nW for the superfluid ^3He experiments under world record rotational speeds up to 12 radian/sec with our first rotating frame.^{63,64} and cryostat⁶⁴.

4.1 Vortex lines penetration experiments in hcp ^4He

With a specially designed rotating cryostat which does not have a 1K pot for the purpose of condensation of circulating ^3He for the dilution refrigerator, experiments under DC rotation have been performed for quite some time.

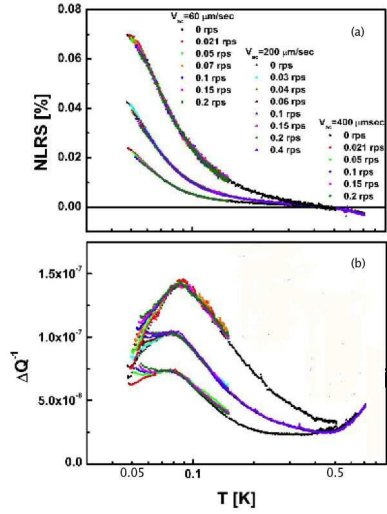


Fig. 10 TO experiments under DC rotation have been performed in the Kubota group for some time^{46,65,66,63,64,60}. $NLRS$ (upper frame (a)) is plotted against T for three AC drive linear velocities at the cell edge under DC rotational velocities indicated in revolution/sec (rps). Details of the actual experiments are described elsewhere⁶⁷. The SS density or $NLRS$ does not change under DC rotation under the present experimental conditions. Evidence of the vortex lines penetration through the sample is given (lower frame (b)) by the change in the energy dissipation under DC rotation at constant velocities as given in the figure below a certain temperature, actually below 75 mK, exactly below T_c , derived from the start of hysteretic behavior^{7,9}. Detailed Ω as well as T dependence analysis will be discussed in the text.

Let us consider how vortex lines penetrating a superfluid can be studied experimentally. We proposed a method for solid ^4He to detect the vortex lines penetration events⁵⁹ by TO technique, detecting extra energy dissipation caused by superflow around the vortex core and the interaction with thermal excitations in the system, similar to the experimental method used for the 3D He film system⁴⁶. From the first evidence for the penetration by vortex lines as presented at the workshop in Trieste⁶⁸, Fig.'s 10(a), (b) show $NLRS$ and ΔQ^{-1} under DC rotation with given rotational speed for three different V_{ac} 's. While $NLRS$ follows the already discussed V_{ac} dependence⁵ it does not change as DC rotational speed changes within the experimental error (see Fig. 10(a)), ΔQ^{-1} data in Fig. 10(b) show a significant change below $T \sim 75$ mK according to the DC angular velocity Ω change for each of three different AC excitation velocities V_{ac} 's. The Ω dependent change in the ΔQ^{-1} does not seem to depend so much on V_{ac} . Fig. 11 shows the almost linear dependence of ΔQ^{-1} for each of temperature T . This behavior certainly supports the picture of the vortex lines in the SS state of hcp ^4He . Let us check if this is right by comparing the expected T dependence of such extra energy dissipation. Following the same analysis as for the 3D He film superfluid⁴⁶, the expected extra energy dissipation caused by the interaction between the superflow around each of the vortex lines and the thermal excitations in the system would be expressed as follows:

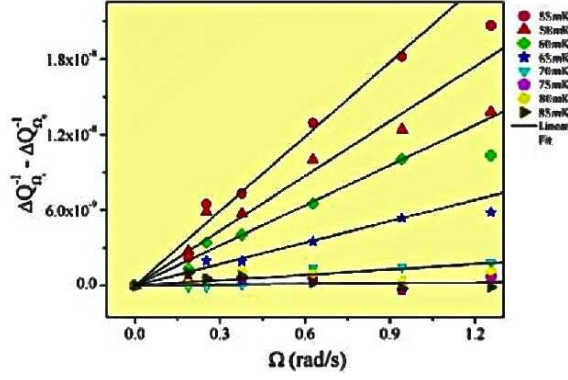


Fig. 11 Ω dependence of the change $\Delta Q_{\Omega}^{-1} - \Delta Q_{\Omega=0}^{-1}$ under DC rotation for the given T s. Ω linear dependence is observed for each T until ≈ 0.9 rad/s rotational speed. The T dependence of the slope in this figure may represent T dependence of the SS density. See text below and the next section. Further detailed analysis according to our experiences^{46,59} is in progress as well.

$$\Delta Q_{\Omega}^{-1} \propto n_v \cdot \rho_{ss}(T) \propto \Omega \cdot \rho_{ss}(T) \quad (4.1)$$

where ΔQ_{Ω}^{-1} is the extra energy dissipation under DC rotation, n_v is the number of vortex lines penetrating the sample, and $\rho_{ss}(T)$ is the SS density, which represents the macroscopic coherence over the whole sample as a function of T . Therefore the simplest idea of its T dependence comes from that of $\rho_{ss}(T)$.

4.2 SS Density $\rho_{ss}(T)$

It is discussed briefly how the value of the SS density $\rho_{ss}(T)$ could be derived from at least two independent experimental quantities, $d\Delta Q_{\Omega}^{-1}/d\Omega$ and $NLRS_{hys}$ in 4.1. Now, how does this appear as evidence for the real supersolidity in hcp solid ${}^4\text{He}$? Fig. 12(a) on the left indicates the slope $d\Delta Q_{\Omega}^{-1}/d\Omega$ of Fig. 11 as a function of T , whereas (b) on the right the hysteretic component $NLRS_{hys}$ discussed in Chapter 3 is displayed. The former is obtained from the data under DC rotation and the other is data obtained without rotation. A significant resemblance between them is observed, namely, both quantities appear below the same temperature near 75 mK and furthermore, linear T dependence below 75 mK continues until some temperature slightly below 57 mK and then increases towards lower T .

It is recalled that the hysteretic component of $NLRS$ has shown a critical behavior as seen in Fig. 7. The critical behavior of the SS density with the critical exponent $2/3$ with $T_c = 56.7$ mK, consistent with 3D XY model, suggests a second order phase transition on one hand, but the existence of the hysteresis implies a first order phase transition. Shimizu *et al.*⁷ have discussed a possible weak first order phase transition as the type of transition from the VF into the SS state⁹ with critical behavior. As has been seen in section 4.2 there is a hint of this kind of transition also in the $\log V_{ac}$ linear dependence jump in the slope as a property of the VF state as in Fig. 8, 9. All these observations tell us that the transition between the VF and the SS states is a unique phase transition. Further study is needed.

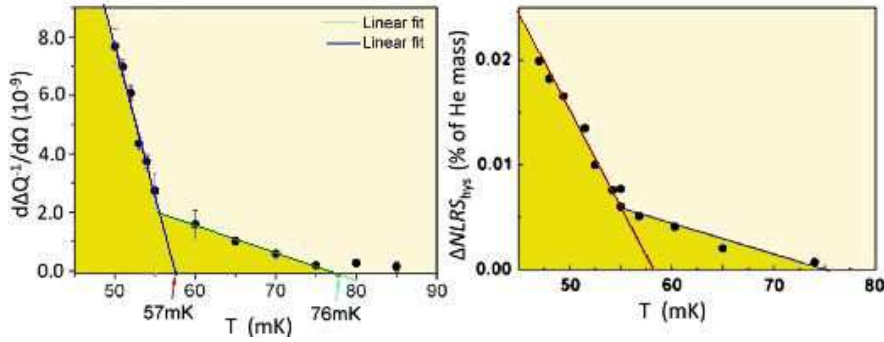


Fig. 12 T dependence of the Ω linear dependent dissipation change under DC rotation for given T 's, compared with the T dependence of the ρ_{ss} obtained by the hysteretic component.

Please note, in Fig. 12, the left hand extra energy dissipation divided by Ω data are taken in the "equilibrium" state under DC rotation, whereas the right hand data of the hysteresis component of $NLRs$ were observed in still condition in an additive manner to the $NLRs$ data from higher T . What does this result mean? The "excited" state is discussed as expelling the external vortices in section 4.1 from the upper section of Fig. 5, where the hysteretic energy dissipation change ΔQ_{hys}^{-1} showed a negative change across the hysteretic path difference between the "excited" and "equilibrium" states. The result expressed on the right side of Fig. 12 indicates that the "excited" state is really a Landau-like state, where external vortices are expelled. The ρ_{ss} is an additive quantity to the VF state $NLRs$.

4.3 The excited state and the equilibrium state

It has been seen that AC vortices are expelled from the "excited" state of hcp ^4He which shows Landau-like state behavior. The vortex lines have been observed to penetrate the "equilibrium" state sample under DC rotation. All these experimental facts show us that the ρ_{ss} is present even in the "equilibrium" state, while the Landau-like state is excited in the hysteretic process below T_c . Then there remains a question whether there is a real Ω_{c1} below which one should expect the real Landau state. Such a question should be answered by future experiments. One may be exciting some shielding current for the "excited" state and the $NLRs$ is increased at the same time as external vortices are expelled.

5 Supporting experimental results by other groups

In this chapter we discuss the consistency of our results and their relation to the results by other groups. The following subjects are discussed, namely, the pressure dependence of the $NLRs$ extrapolated to $T = 0$ K, the specific heat anomaly observed around 75 to 100 mK by Chan's group and the superflow experiments by Ray and Hallock next, and then TO experiments on "ultra pure" or single crystal samples with "onset" near 60 to 79 mK.

Pressure dependence of $NLRS$ as $T \rightarrow 0K$: One of the most important properties to check consistency with results by other groups is the absolute size of the $NLRS$ extrapolated to $T = 0 K$ $NLRS_0$, since Rittner and Reppy⁵¹ reported a huge change of $NLRS_0$ according to the sample cell geometry, namely to the ratio between surface area and the volume of the solid 4He sample. The present author thinks that their findings might include some effects of viscoelasticity. In any case it is important to quote some characteristic property to identify the sample studied. Kubota group data, except for the earliest ones in a cell with slightly complicated geometry⁶⁹, all show rather low $NLRS_0$ and are stable during repeated measurements over a period exceeding a year, as in Penzev *et al.*⁵.

Specific heat anomaly at 75 -100 mK: A phase transition of second kind with critical fluctuations would cause a sharp specific heat peak and that of first kind would produce a jump in the specific heat. There have been serious searches by Chan's group and they reported a definite specific heat peak at $T \approx 75-100$ mK, independent of a small 3He content^{70,71}. One does not yet know the detailed connection to the transition from the VF state into the SS state, but the observation of the transition into SS state from the VF state is consistent with the specific heat peak reported by Lin *et al.*^{70,71}.

Super flow experiments: While earlier attempts to observe DC super flow failed^{72,73}, recent flow experiments utilizing the thermomechanical effect with liquid in porous Vycor to drive the bulk solid He mass flow by Ray and Hallock⁷⁴ seem to have some correspondence to our observation of the VF and the transition into the SS states^{7,8,9}. Actually they claim to have observed mass flow below ~ 600 mK and some drastic change below ~ 70 mK and increase of the mobility below this T . Theoretical consideration by Aleinikava, Dedits, and Kuklov⁷⁵ describes a microscopic picture of glide and superclimb of dislocations to explain the above experiment.

Ultra pure, single crystal samples experiments: Another interesting observation, which was made for solid 4He samples near 60mK, is reported by Clark, West and Chan⁷⁶. They have grown large crystals with high purity and compared them to standard, pure 4He samples with various qualities. The onset temperature for a number of samples with constant temperature or constant pressure crystallization collapse onto a single value of $\sim 79 \pm 5$ mK and the low temperature part is well fitted with what they call the $NCRI$, which is proportional to $(1 - T/T_c)^\gamma$, where $\gamma = 2/3$ with $T_c = 0.06$ K. It looks as if the purest (single crystal) samples with smallest amount of imperfections would not have the VF contribution, but only the SS part. The absolute size of their $NLRS$ beyond 0.2 % is still much larger than our observation for $NLRS$ or ρ_{ss} (see Fig. 6). Nobody yet knows the relation between their results and the VF to SS transition. It is interesting to see a 3D XY critical behavior for their purest samples. It is important to ask the relative size of the VF state and the SS state contributions to the observable $NLRS$.

6 Summary and Discussion

Results for the VF state and the SS state in hcp 4He are summarized as follows:

- 1]. The VF state was found below $T_o \sim 500$ mK. The VF state is characterized by the dynamics of the vortex tangle and its cessation at 30mK.
- 2]. The transition from the VF state into the SS state is marked by a) appearance of

hysteresis below T_c with evolution of the equilibrium state and the excited state, b) the VF state $\log V_{ac}$ linear dependence change in the equilibrium state at T_c .

3]. Vortex lines penetration in the equilibrium state under DC rotation has been detected by the extra energy dissipation signal under rotation. The extra dissipation was found to follow the expected relation (4.1) and its temperature dependence was found to coincide with the SS density $\rho_{ss}(T)$, which was derived from the proposed quantity of the hysteretic component of the $NLRS$, $NLRS_{hys}$.

4]. The excited state was discussed to be rejecting external vortices totally and this would lead to a consistent picture of a Landau-like state with 3].

5]. The critical velocity $V_c(T=0)$ is evaluated to be about 1 cm/s from the $\log V_{ac}$ linear dependence of the hysteretic component $NLRS_{ac}$ to the extrapolated value for $NLRS_{ac}=\rho_{ss}=0$. This is in reasonable agreement with the evaluation $V_c=h/(m_4 \xi_0 \pi)$ = 6-12 cm/s for $\xi_0=25-50$ nm.

The evidence of the VF state and its transition into the SS state has been shown. It requires some different mechanism than the BCS scenario. The VF triggering SS state appearance is happening, where the VF state is describable by a tangled vortex state model probably involving some thermally excited low dimensional subsystems. The macroscopic coherence appearance at low T well below T_c should be related to the problem of the ground state discussed by Anderson⁷⁷. The shear modulus observation^{39,40} problem has been so far neglected, but it would be essential to construct a real microscopic description of the supersolidity and the vortex state in hcp ^4He . So far the vortex physics in solid ^4He has been discussed in the VF state and the SS state, in one of the simplest Bose quantum crystals. Before solid ^4He the vortex state had been discussed only among so called "new type of superconductors"⁴². Then, one may ask a question: is hcp ^4He a high temperature superfluid? It would be a fundamental question of the present day understanding of superfluidity, superconductivity and the vortex state, related to the next question. Are there further new supersolids awaiting discovery? After studying the case of hcp ^4He , one may ask oneself such a question. It would be a new challenge to find one in the second century following the first production of a superfluid about a century ago.

Acknowledgements Our own developments with higher stability TO experiments under rotation involve decades of the following people's efforts after the initial TO cooperation involving Takashi Watanabe, Nobuo Wada, and Keiya Shirahama: Takeshi Igarashi, Goh Ueno, Takeshi Iida, Vladimir Kovacic, Maxim Zalalutdinov, Muneyuki Fukuda, Toshiaki Obata, Vitaly Syvokon, Nikoley Mikhin, Itsumi Tanuma, Yuji Ito, Ken Izumina, Andrei Penzev, Yoshinori Yasuta, Nobutaka Shimizu, Akira Kitamura, and Masahiko Yagi. Contributions are appreciated by other members of Kubota group in the development and technical support by Hisahiro Hamada of Kohzu Seiki co., Masahito Sawano, Kiyoshi Akiyama of Rigaku co. Cooperation with J.D. Reppy, and Kris Rogacki and theoretical support by Edoard Sonin, Tomoki Minoguchi, and Sergey Nemirovskii has been indispensable. The author thanks Robert Mueller for the continued encouragement and for correction in the author's English expressions over the whole period.

References

1. E. Kim and M. H. W. Chan. *NATURE*, 427:225–227, 2004.
2. E. Kim and M. H. W. Chan. *science*, 305:1941, 2004.
3. P. W. Anderson. *Nature Physics*, 3:160 – 162, 2007.
4. P. W. Anderson. *Phys. Rev. Lett.*, 100:215301–1–3, 2008.
5. A. Penzev, Y. Yasuta, and M. Kubota. *Phys. Rev. Lett.*, 101:065301, 2008.
6. S. K. Nemirovskii, N. Shimizu, Y. Yasuta, and M. Kubota. arxiv:0907.0330.
7. N. Shimizu, Y. Yasuta, and M. Kubota. arxiv:0903.1326, 2009.
8. M. Kubota, N. Shimizu, Y. Yasuta, P. Gumann, and S. K. Nemirovskii. *J. Low Temp. Phys.*, 158:572–577, 2010.
9. M. Kubota, N. Shimizu, Y. Yasuta, A. Kitamura, and M. Yagi. *J Low Temp Phys*, 162:483–491, 2011.
10. L. Reatto and G. V. Chester. *Phys. Rev.*, 155(1):88 – 100, 1967.
11. G. V. Chester. *Phys. Rev. A*, 2(1):256–258, 1970.
12. A. F. Andreev and I. M. Lifshitz. *JETP*, 29:1107–1113, 1969.
13. A. J. Leggett. *Phys. Rev. Lett.*, 25(22):1543–1546, 1970.
14. H. Matsuda and T. Tsuneto. *Progress of Theoretical Physics*, Supplement,(46):411– 436, 1970.
15. J. G. Bednorz and K. A. Mueller. *Z. Phys.*, 64:189, 1986.
16. P. W. Anderson. *Rev. Mod. Phys.*, 38(2):298–310, 1966.
17. F. London. *Phys. Rev.*, 34:947–954, 1938.
18. J. Bardeen, L. N. Cooper, and J. R. Schrieffer. *Phys. Rev.*, 108:1175, 1957.
19. Feynmann. volume 1 of *Progress in Low Temperature Physics*. North-Holland, Amsterdam, 1955.
20. Garry A. Williams. *Phys. Rev. Lett.*, 59(17):1926 – 1929, 1987.
21. G. Blatter, M. V. Feigel'man, V. B. Geshkenbein, A. I. Larkin, and V. M. Vinokur. *Rev. Mod. Phys.*, 64(4):1125–1388, 1994.
22. Y. Kamihara and et al. *J. Am. Chem. Soc.*, 128:10012–10013, 2006.
23. D. S. Fisher, M. P. A. Fisher, and D. A. Huse. *Phys. Rev. B*, 43(1):130, 1991.
24. J. R. Clem, Thomas Pe, and M. Benkraud. *Physica C*, 282-287:311, 1997.
25. P. W. Anderson. Theory of supersolidity. arXiv:1111.1707, pages 1–15, 2011.
26. V. L. Berezinskii. *Sov. Phys. JETP*, 34:610, 1972.
27. J. M. Kosterlitz and D. J. Thouless. *J. Phys.*, c 5:L124, 1972.
28. D. R. Nelson and J. M. Kosterlitz. *Phys. Rev. Lett.*, 39(19):1201–1205, 1977.
29. D. J. Bishop and J. D. Reppy. *Phys. Rev. Lett.*, 40(26):1722–1730, 1978.
30. D. Bishop and J. Reppy. *Phys. Rev. B*, 22:5171, 1980.
31. Vinary Ambegaokar, B. I. Halperin, David R. Nelson, and Eric D. Siggia. *Phys. Rev. B*, 21(5):1806–1825, 1980.
32. Minoru Kubota. *J Low Temp PhysL*, 2012.
33. S. I. Shevchenko. *Sov. J. Low Temp. Phys.*, 13:61, 1987.
34. S. I. Shevchenko. *Sov. J. Low Temp. Phys.*, 14:553, 1988.
35. Nikolay Prokf'ev. *Advances in Physics*, 56(2):381–402, 2007.
36. D. Galli and L. Reatto. *J. Phys. Soc. JPN*, 77(11):111010–1–16, 2008.
37. S. Balibar and F. Caupin. *J. Phys.: Condens. Matter*, 20:173201–1–19, 2008.
38. Sebastien Balibar. *Nature*, 464:176 – 182, 2010.
39. James Day and John Beamish. *Nature*, 450:853 – 856, 2007.

-
40. J. T. West, O. Syshchenko, J. Beamish, and M. H. W. Chan. *Nature Physics*, 5:598 – 601, 2009.
 41. Yuyu Wang, Lu Li, M. J. Naughton, G. D. Gu, S. Uchida, and N. P. Ong. *Phys. Rev. Lett.*, 95:247002–1–4, 2005.
 42. A. J. Leggett. *Quantum Liquids*. Oxford University Press, 2006.
 43. E. Kim and M. H. W. Chan. *Phys. Rev. Lett.*, 97:115302–1–4, 2006.
 44. J. D. Reppy and A. Tylar. *Excitations in Two Dimensional and Three Dimensional Quantum Fluids*, volume 291-300. Plenum Press, New York, 1991.
 45. M. Fukuda. PhD thesis, Dept. Physics, the university of Tokyo, 1999.
 46. M. Fukuda, M. K. Zalalutdinov, V. Kovacik, T. Minoguchi, T. Obata, M. Kubota, and E. B. Sonin. *Phys. Rev. B*, 71:212502, 2005.
 47. M. Tsubota, C. Barenghi, T. Araki, and Mitani A. *Phys. Rev. B*, 69:134515, 2004.
 48. S. K. Nemirovskii. *Phys. Rev. B*, 81:064512, 2010.
 49. Y. Aoki, J. C. Graves, and H. Kojima. *Phys. Rev. Lett.*, 99:015301–1–4, 2007.
 50. A.C. Clark, J.D. Maynard, and M.H.W. Chan. *Phys. Rev. B*, 77:184513, 2008.
 51. Ann S. Rittner and John D. Reppy. *Phys. Rev. Lett.*, 101:155301–1–4, 2008.
 52. D. J. Josephson. *Phys. Lett.*, 21:608, 1966.
 53. M. E. Fisher, M. N. Barber, and D. Jasnow. *Phys. Rev. A*, 8:1111–, 1978.
 54. N. P. Mikhin, V. E. Syvokon, T. Obata, and M. Kubota. *Physica B*, 329–333:272–273, 2003.
 55. P.W. Anderson. private communication, June 2011.
 56. G. B. Hess and W. M. Fairbank. *Phys. Rev. Lett.*, 19(5):216–218, 1967.
 57. T. Obata, I. Tanuma, T. Igarashi, and M. Kubota. *J. Low Temp. Phys.*, 138(3/4):929–932, 2005.
 58. K. Shirahama, M. Kubota, S. Ogawa, N. Wada, and T. Watanabe. *Phys. Rev. Lett.*, 64(13):1541–1544, 1990.
 59. M. Kubota, M. Fukuda, T. Obata, A. Ito, A. Penzev, T. Minoguchi, and E. B. Sonin. *AIP Conf Proc*, 850:283–284, 2006.
 60. M. Yagi, A. Kitamura, N. Shimizu, Y. Yasuta, and M. Kubota. *J Low Temp Phys*, 162:754–761, 2011.
 61. R. Ishiguro and *et al.*. *Phys. Rev. Lett.*, 93(12):125301–1–4, 2004.
 62. M. Yamashita and *et al.*. *Phys. Rev. Lett.*, 94:075301 –1–4, 2005.
 63. V. Kovacik, M. Fukuda, T. Igarashi, T. Torizuka, M. K. Zalalutdinov, and M. Kubota. *J Low Temp Phys*, 101(3/4):567–572, 1995.
 64. M. Kubota and *et al.* *Physica B*, 329-333:1577–1581, 2003.
 65. M. Fukuda, M.K. Zalalutdinov, V. Kovacik, T. Igarashi, T. Obata, K. Ooyama, and M. Kubota. *J Low Temp Phys*, 113(3/4):417 – 422, 1998.
 66. M Kubota, G Ueno, T Igarashi, and Y Karaki. *Physica B*, 194-196:797, 1994.
 67. M. Yagi, A. Kitamura, N. Shimizu, Y. Yasuta, and M. Kubota. *J Low Temp Phys*, 162:492–499, 2011.
 68. Trieste August 2008.
 69. A. Penzev, Y. Yasuta, and M. Kubota. *J Low Temp Phys*, 148:677–681, 2007.
 70. X. Lin, A.C. Clark, and M.H.W. Chan. *nature*, 449:1025
 71. X. Lin, A. Clark, Z. Cheng, and M.H.W. Chan. *Phys. Rev. Lett.*, 102:125302, 2009.
 72. J. Day, T. Herman, and J. Beamish. *Phys. Rev. Lett.*, 95:035301, 2005.
 73. J. Day and J. Beamish. *Phys. Rev. Lett.*, 96:05304, 2006.

-
74. M. Ray and R. Hallock. *Phys. Rev. Lett.*, pages 145301–1–4, 2010.
 75. D. Aleinikava, E. Dedits, and A. Kuklov. *J Low Temp Phys*, 162:464, 2011.
 76. A.C. Clark, J.T. West, and M.H.W. Chan. *Phys. Rev. Lett.*, 99:135302, 2007.
 77. P. W. Anderson. *arXiv:1102.4797*, 2011.